Microstructure and permeability of anisotropic open-cell foams

Van Hai TRINH [1(✉)]

[1] Le Quy Don Technical University (LQDTU), Hanoi 10000, Vietnam
hai.tv@lqdtu.edu.vn

Abstract. Solid foams within open-cell structure have been used widely in mechanical, thermal and acoustical applications due to their functional properties such as lightweight, high surface area-to-volume ratio. The present paper investigates numerically the effect of microstructural properties of anisotropic random foams on the permeability. To this regard, we first employ molecular dynamics simulation to generate the Representative Volume Element (RVE) based on Voronoi tessellation, the RVEs presenting the structure of random foams are then used to compute the foam permeability behavior by solving the viscous problem. The obtained results reveal that the finite element computations agree well with both reference analytical model and experimental data. The anisotropy degree has a significant effect on the permeability of foams.

Keywords: Anisotropic, open-cell, random foam, microstructure, permeability.

1 Introduction

The problems raised in transport phenomena in natural and man-made media have been attracted the growing attention of both industrialists and scientists from many engineering disciplines (e.g., geophysics, acoustics, thermal engineering). In which, understanding of permeability behavior of porous material provides the fundamentals (i.e., fluid flow and heat transfer) for industrial and environmental processes [1]. From various studies over several decades, it can be stated that the permeability is a highly variable parameter according to the basic morphological parameters such as pore size and solid volume fraction [1-6]. Due to the importance of permeability, such parameter of various porous media (e.g., foam [4-6], granular [1, 2], fibrous [7]) is characterized by numerous approaches: analytical model [3], semi-empirical law [8], experimental [4-6] or numerical [1, 2] curve-fitting.

Analytical models even for highly idealized morphologies often require adjustable factors or limitations the range of geometrical parameters. Similarly, performing a large number of experiments on various series of real samples is a hard task in terms of the consumption. Contrary, numerical approach as testing on virtual material samples allows us to design structures having derived functional properties.

In this paper, we employ the numerical method for predicting permeability behavior of isotropy and anisotropy open-cell foams.

2 Microstructure modeling of random open-cell foams

In a Voronoi pattern, the partitioning is based on a set of seed points distributed in a model space where each cell is defined by all points that are closer to one particular seed point than to any others. Mathematically, given a set S of N points in a three-dimensional space, the process of associating all the locations of the space into polyhedral regions with the closest point of S is called Voronoi partitioning process. The polyhedral regions are called cells. The union of all the cells is then referred to as a Voronoi diagram. Theoretically, a Voronoi diagram may be constructed in any dimensional space. A cellular foam model based on Voronoi partitions of 3D space is built as follows [9]. First, a set of N nuclei (seed points) is given in a three-dimensional finite space R^3. For each nucleus, let cell V_i be the region consisting of all locations in the space which are closer to P_i than any other nucleus P_j (with $j \neq i$), a cell V_L corresponding to seed point P_i is defined as:

$$V_L(\boldsymbol{x}_i) = \left\{ \boldsymbol{x} \in R^3 \;\middle|\; \|\boldsymbol{x} - \boldsymbol{x}_i\| \leq \|\boldsymbol{x} - \boldsymbol{x}_j\| \;\; \forall i \neq j \right\} \tag{1}$$

where $\boldsymbol{x}_i$ and $\boldsymbol{x}_j$ are respectively the coordinates of seed points P_i and P_j.

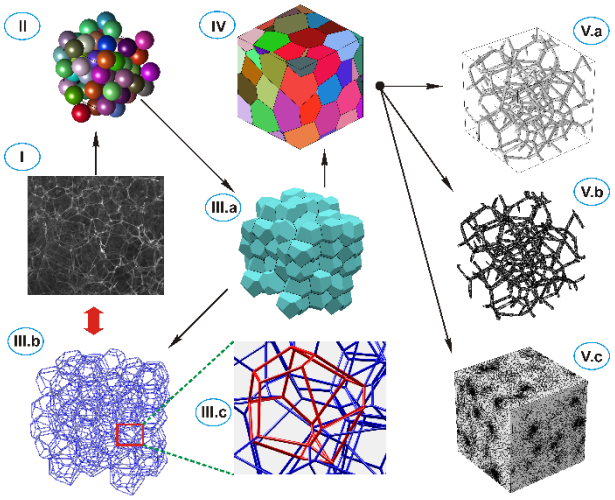

Fig. 1. Schematic diagram of major steps in the procedure for generating random open-cell foam structures: SEM image of real foam (I); assembly of randomly close sphere packing (II); Voronoi cell pattern (III.a) reconstructed structure of open foam with cylindrical structs (III.b) and detail of a typical polyhedron (III.c); various periodic REVs and the FE meshes (IV, V).

Each seed point is surrounded by a cell that contains all points in space that are closer to this particular seed point than to any other. Consequently, cell walls will appear centrally aligned on, and perpendicular to, lines that fictively connect two neighbor seed points. Cell edges appear wherever cell walls intersect and cell vertices appear where cell edges intersect (see Fig. 1(III)). The result is strictly convex cells with flat

faces. An ordered set of seed points can be used for creating ordered and regular structures, for instance, structures made of Kelvin or Weaire-Phelan pattern. Voronoi algorithm generates around each seed a convex polyhedral unit cell made of vertices, joined by edges delimiting planar faces, which connect neighbor cells. Finally, a foam skeleton is completely established (see Fig. 1(III.a)). The corresponding finite mesh models of skeleton and pore domain are graphed in Fig. 1(V.c) and 1(V.c). From this, both isotropic and anisotropic foam material is studied by the virtual REV. The anisotropic virtual REV is construction by elongating and compressing in *x*-directions and *z*-direction by a factor R_A and $1/R_A$ respectively while the *y*-direction is kept (Fig. 2).

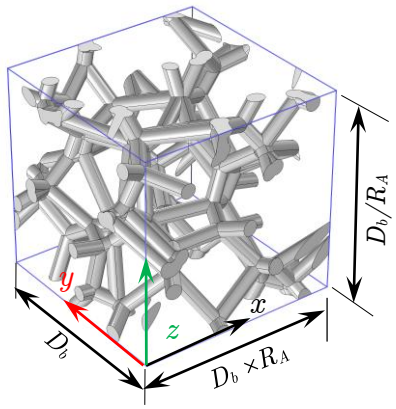

Fig. 2. REV configuration with an introduction of the ratio of anisotropy R_A.

3 Permeability predicting of anisotropic foams

The low Reynolds number flow of an incompressible Newtonian fluid is governed by the usual Stokes equations in the fluid phase [10]:

$$\eta \Delta \mathbf{v} - \nabla p = -\boldsymbol{G} \quad \text{with} \quad \nabla . \mathbf{v} = 0 \quad \text{in} \quad \Omega_f \tag{2}$$

where $\boldsymbol{G} = \nabla p^{\mathrm{m}}$ a macroscopic pressure gradient acting as a source term. $\mathbf{v}$, p, and η denote respectively the velocity, pressure, and viscosity of the fluid. The velocity field $\mathbf{v}$ satisfies the no-slip condition ($\mathbf{v} = 0$) at the fluid-solid interface, $\partial\Omega$.

According to the Darcy law, fluid permeability tensor $\boldsymbol{K}$ is determined from the average velocity vector over the whole microstructure and the macroscopic pressure gradient as $\langle \mathbf{v} \rangle = -(1/\eta)\, \boldsymbol{K} \cdot \boldsymbol{G}$, this could be expressed in three-dimensional space,

$$\begin{bmatrix} \langle x \rangle \\ \langle y \rangle \\ \langle z \rangle \end{bmatrix} = -\frac{1}{\eta} \begin{bmatrix} K_{xx} & K_{xy} & K_{xz} \\ K_{yx} & K_{yy} & K_{yz} \\ K_{zx} & K_{zy} & K_{zz} \end{bmatrix} \begin{bmatrix} G_x \\ G_y \\ G_z \end{bmatrix} \tag{3}$$

Finally, nine components (K_{ij}) of the permeability tensor could be estimated by solving Eq. (3) within three independent steps with a pressure gradient that is applied

only the considered direction (e.g., by applying the gradient $\boldsymbol{G} = [G_x\ 0\ 0]^T$ in the x-direction, three left coefficients K_{xx}, K_{yx} and K_{zx} of the permeability tensor is deduced, see Fig .3 for the obtained solution fields of local permeability components).

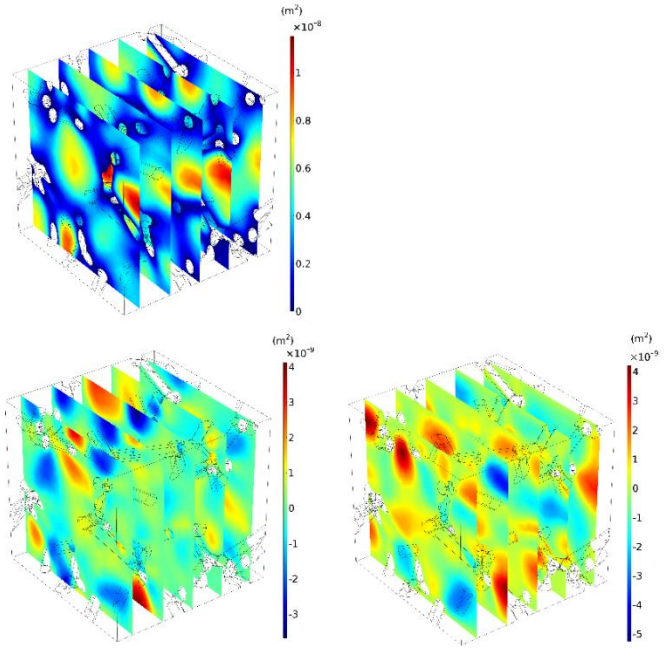

Fig. 3. The solution fields of local permeability components correspond to the applied gradient $\boldsymbol{G} = [G_x\ 0\ 0]^T$. The results are for: $x\eta/G_x$ (upper), $y\eta/G_x$ (lower, left) and $z\eta/G_x$ (lower, right).

4 Results and discussion

In this section, a foam structure configuration proposed in Ref. [2] is used to validate our numerical procedure (e.g., based the perfect Kelvin pattern with a cell size of 4 mm and a porosity of 0.786). At the same time, the effect of anisotropy level on the regular foam permeability is investigated. Firstly, applying the numerical procedure presented in Sec. 3, we obtain a fully symmetric permeability tensor of isotropy structure ($R_A = 1$) as $\boldsymbol{K} = \text{diag}(8.32, 8.32, 8.32)\times10^{-8}$ (m^2). As shown in Fig. 4, the numerical obtained results of the permeability tensor is in very good agreement with the reference data proposed in Ref. [2], which validates our finite element model, the present smooth curve shows also the better stable and convergence property of our numerical model. In term of permeability, it is seen that (i) for $R_A \in [1, 1.6]$, within increasing of R_A, the x-direction permeability increases, while the x-direction and y-direction permeability decrease; (ii) for $R_A \in [1.6, 3]$, all permeability components decrease due to the increase of the specific surface area or the effect of strut shape [2].

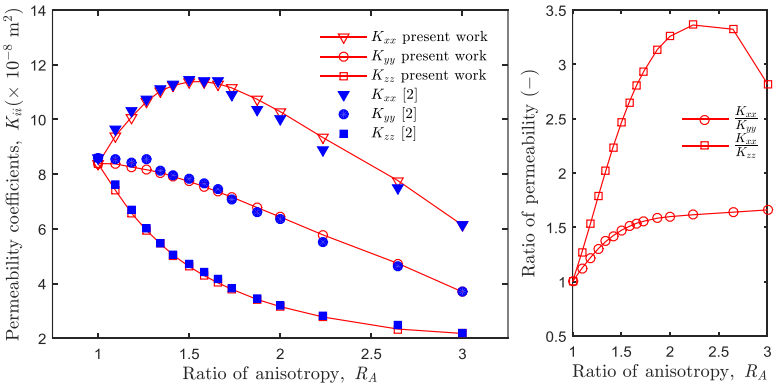

Fig. 4. Permeability tensors diagonal components (left) and their relative ratio (right) versus ratio of anisotropy.

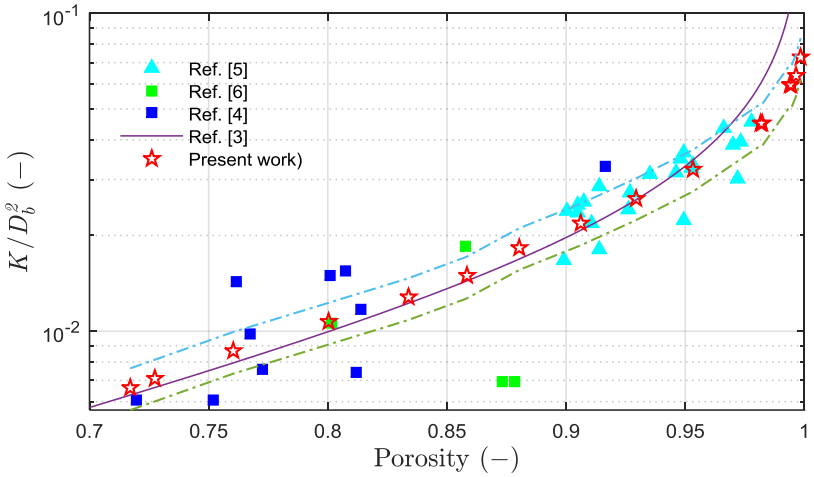

Fig. 5. Dependence of permeability on porosity and pose size of open-cell foams.

Fig. 5 compares the permeability of random foam materials obtained from different approaches, it can be seen from the numerical present results (star makers) that our computations are in good agreement both with analytical model [3] and experimental data [4-6] of the static permeability in the whole porosity ranging from 0.70 to 0.99. Interestingly, compared to the analytical law, our permeability predictions show a better fitting with measurements for highly porous foams (i.e., with porosity > 96%). By considering the anisotropic foam materials having the relative ratio (e.g., 15 %) of their permeability components, as seen from the permeability zone created by two dash lines (for +15 % and −15 %) that the proposed numerical modeling of random open-cell foam within an anisotropic factor enables to capture the static permeability behavior of real structures.

5 Conclusion

This paper presents the microstructure-based approach to characterize numerically the relationship between local geometrical information and permeability behavior of random anisotropic open-cell foams. The proposed method is validated by its accuracy and robustness in compared with existing experimental data and analytical model in term of determining components of permeability tensors for both regular and irregular foam structures. As demonstrated, the fluctuation of experimental permeability of real foams can be explained by the effects of the ratio of anisotropic. Our numerical modeling of random open-cell foam within an anisotropic factor enables to capture the static permeability behavior of real structures in a wide range of porosity.

The potential application of this work relies on not only modeling the foamy permeability parameter but also other important transport behaviors of mass and heat.

References

[1] C. Boutin and C. Geindreau, "Estimates and bounds of dynamic permeability of granular media," *The Journal of the Acoustical Society of America,* vol. 124, pp. 3576-3593, 2008.

[2] Y. Jobic, P. Kumar, F. Topin, and R. Occelli, "Determining permeability tensors of porous media: A novel 'vector kinetic' numerical approach," *International Journal of Multiphase Flow,* vol. 110, pp. 198 - 217, 2019.

[3] X. Yang, T. J. Lu, and T. Kim, "An analytical model for permeability of isotropic porous media," *Physics Letters A,* vol. 378, pp. 2308-2311, 2014.

[4] G. I. Garrido, F. Patcas, S. Lang, and B. Kraushaar-Czarnetzki, "Mass transfer and pressure drop in ceramic foams: a description for different pore sizes and porosities," *Chemical Engineering Science,* vol. 63, pp. 5202-5217, 2008.

[5] A. Bhattacharya, V. Calmidi, and R. Mahajan, "Thermophysical properties of high porosity metal foams," *International Journal of Heat and Mass Transfer,* vol. 45, pp. 1017-1031, 2002.

[6] J. Richardson, Y. Peng, and D. Remue, "Properties of ceramic foam catalyst supports: pressure drop," *Applied Catalysis A: General,* vol. 204, pp. 19-32, 2000.

[7] M. Hunt and C. Tien, "Effects of thermal dispersion on forced convection in fibrous media," *International Journal of Heat and Mass Transfer,* vol. 31, pp. 301-309, 1988.

[8] O. Doutres, N. Atalla, and K. Dong, "Effect of the microstructure closed pore content on the acoustic behavior of polyurethane foams," *Journal of Applied Physics,* vol. 110, p. 064901, 2011.

[9] A. Okabe, *Spatial tessellations*: Wiley Online Library, 1992.

[10] M. Avellaneda and S. Torquato, "Rigorous link between fluid permeability, electrical conductivity, and relaxation times for transport in porous media," *Phys. Fluids A-Fluid,* vol. 3, pp. 2529-2540, 1991.